Advanced Thermoelectric Power System Investigations for Light-Duty and Heavy Duty Applications: Part II

Terry J. Hendricks
Jason A. Lustbader
National Renewable Energy Laboratory
Center for Transportation Technology & Systems
1617 Cole Boulevard, M.S. 1633
Golden, CO 80401 USA
e-mail: terry_hendricks@nrel.gov

ABSTRACT

Part II of this two-part paper leverages off the findings in Part I describing the mathematical basis and system modeling approach used in thermoelectric power generation (TEPG) investigations for waste heat recovery in light-duty passenger (LDP) and heavy-duty (HD) vehicles. The TEPG sytsem model has been used to: (1) investigate the behavior and interdependence of important thermal and TEPG design parameters, and (2) compare potential TEPG system power output for a variety of thermal conditions in LDP and HD vehicles. Integrated system modeling and analyses have been performed for: 1) LDP conditions of T_{exh} = 700 °C (973 K) and $\dot{m}_h$ = 0.01, 0.02, and 0.03 kg/sec, and 2) HD conditions of T_{exh} = 512 °C (785 K) and $\dot{m}_h$ = 0.2, 0.3, and 0.4 kg/sec. Analysis results, TEPG design parameter behavior, thermoelectric (TE) material effects, and interdependence of critical thermal / TE system design parameters are discussed. Interaction of heat exchanger performance and TEPG device performance creates critical system impacts and performance dependencies, which maximize TEPG system power outputs and create preferred heat exchanger and TEPG performance regimes. Part II demonstrates the integrated system analysis approach to heat exchanger / TEPG system performance, allowing NREL to simultaneously quantify these critical system design effects in LDP and HD vehicles. HD vehicle analysis results also indicate that 5-6 kW of electrical energy production is possible using HD vehicle exhaust waste heat.

NOMENCLATURE

English

A_p - p-type element area [m^2]
A_n - n-type element area [m^2]
I - Device current [A]
L - TE element length [m]
$\dot{m}_c$ - Cold-side (Ambient) mass flow rate [kg/sec]
$\dot{m}_h$ - Hot-side (Exhaust) mass flow rate [kg/sec]
N - Number of couples
P - Device power [W]
q - Hot side or cold side thermal energy transfer [W]
R_{th} – Hot-side or cold-side thermal resistance [K/W]
T_{amb} – Ambient temperature [K]
T_{exh} – Exhaust gas temperature [K]
T_h - TE hot side temperature [K]
T_c - TE cold side temperature [K]
UA - Effective Heat Exchanger Conductance * Area [W/K]
V - Device voltage [V]

Greek

ΔT_c – Cold side temperature difference [$T_c - T_{amb}$] [K]
ε_c - Cold-side heat exchanger effectiveness
ε_h - Hot-side heat exchanger effectiveness
η - Thermoelectric conversion efficiency
σ - Heat loss factor – percentage of interface input heat

Subscripts

c - Cold-side of TE device
h - Hot-side of TE device
ex - Refers to hot or cold side heat exchanger
TE - TE device
pk - Peak power conditions

INTRODUCTION

Part I of this paper discusses the vehicle waste heat recovery motivations and system requirements being sought by the U.S. Department of Energy (DOE) and the National Renewable Energy Laboratory (NREL). Light duty passenger (LDP) vehicle exhaust systems operating at gas temperatures from 500°C up to 900°C, and in heavy-duty (HD) vehicle exhaust systems operating at gas temperatures of 500°C to 650°C, provide significant opportunities for and benefits from waste thermal energy recovery. Part I discusses the advanced, next-generation thermoelectric (TE) materials developed in the past 5 years that are providing enhanced opportunities for thermoelectric power generation (TEPG) systems with much higher TE conversion efficiencies and power outputs, and the promise of cost-effective waste thermal energy conversion in advanced vehicle systems. However, TE materials research is only one aspect of the entire picture surrounding development of a TEPG system that integrates with a LDP or HD vehicle. NREL is therefore investigating system power benefits and thermal integration challenges of using TEPG systems with various advanced, next-generation TE materials, such as skutterudites (p-type $CeFe_4Sb_{12}$; n-type $CoSb_3$), quantum-well materials, and thin-film superlattice materials, to recover waste thermal energy at various potential locations within LDP vehicles and HD trucks. Optimum design analyses were continued for three advanced TE material combinations in three segmented-leg TE design configurations:

1) p-type $CeFe_4Sb_{12}$ / p-type Bi_2Te_3; n-type $CoSb_3$ /n-type Bi_2Te_3 [1]
2) p-type TAGS / p-type Bi_2Te_3; n-type 2NPbTe / n-type Bi_2Te_3 (Hi-Z Technology, Inc.)
3) p-type $CeFe_4Sb_{12}$ / Zn_4Sb_3 / p-type Bi_2Te_3; n-type $CoSb_3$ / n-type Bi_2Te_3 [1]

with the intention of more clearly defining the TEPG operating regimes and design characteristics.

TE SYSTEM DESIGN CHARACTERISTICS IN LIGHT DUTY VEHICLE APPLICATIONS

Part I of this paper discussed the power output and device efficiency characteristics in exhaust waste heat recovery near the catalytic converter in LDP vehicles. This section continues that discussion by focusing on TE device design characteristics associated with this application.

Optimum Device Design Characteristics

Optimum TE design parameters obtained in these systems analyses include the p-type and n-type leg cross-sectional areas, the segment lengths in each leg, and the number of couples for the optimum TE system designs. These optimum TE design characteristics provide important information on design requirements to achieve required system power and efficiency levels.

Figure 1 shows the p-type cross-sectional area requirements as a function of T_h and T_c for a 42-volt TE system using TE material set #1 and an exhaust gas temperature of 973 K. Figure 2 shows the n-type cross-sectional area requirements as a function of T_h and T_c for a 42-volt TE system using TE material set #1 and an exhaust gas temperature of 973 K. The p-type area requirements are generally lower than the n-type area requirements for common conditions in the 42-volt TE system designs shown in Figures 1 and 2. This is, of course, a ramification of the electrical resistivity and thermal conductivity properties (and their differences) in the p-type and n-type materials in TE material set #1. In general, Figs. 1 and 2 show cross-sectional area requirements increasing sharply as hot side mass flow rate, $\dot{m}_h$, increases, creating larger hot side thermal flow into the device. Cross-sectional area also increases dramatically as T_h decreases. This creates important system design considerations when designing waste energy recovery TEPG systems in LDP and HD vehicles.

Optimized p-leg and n-leg cross-sectional areas were also established for 42-volt systems using TE material set #3 (3-p segment/2-n segment). Due to space limitations it is not possible to present this data, but the general trends are the same as those shown in Figures 1 and 2. In general, the optimum p-leg and n-leg area requirements were larger using TE material set #3 due to material property differences.

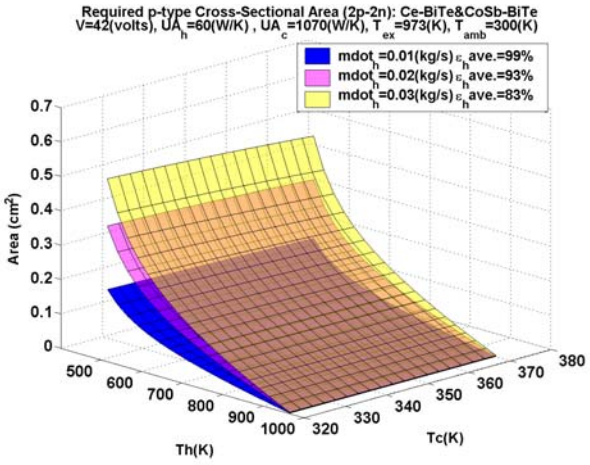

Figure 1 – Optimized p-Type Leg Cross-Sectional Area for 42-Volt TE System Using TE Material Set #1.

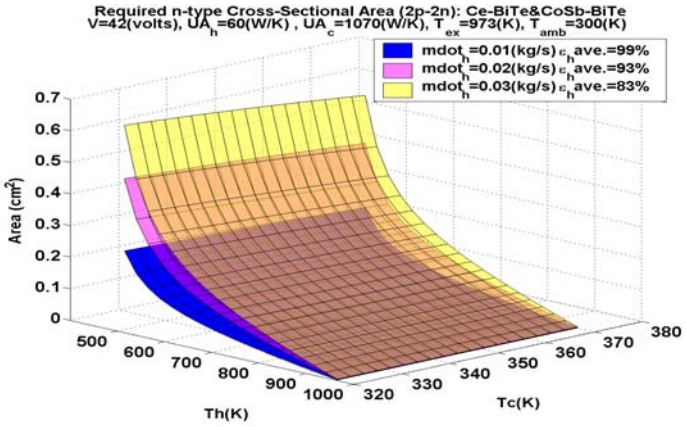

Figure 2 – Optimized n-Type Leg Cross-Sectional Area for 42-Volt TE System Using TE Material Set #1.

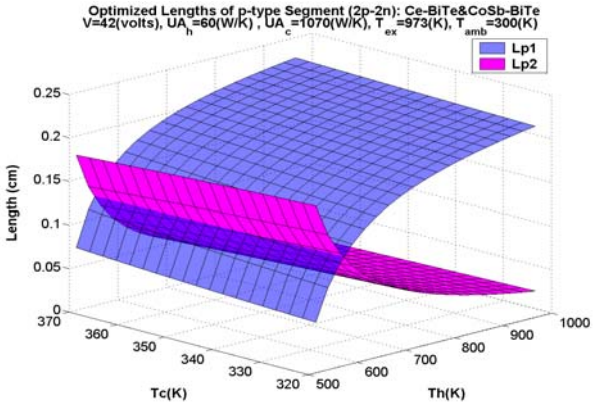

Figure 3 - Optimized p-Type Material Lengths for TE Material Set #1 in a 42-Volt TE Device & T_{exh} = 973 K.

A critical device design characteristic is the optimized lengths of each material segment in the p-type and n-type TE legs. The 42-volt design analysis using TE material set #1 and an exhaust gas temperature of 973 K was performed assuming a total element leg length of 0.25 cm. Figure 3 displays the optimized p-type material segment lengths as a function of T_h and T_c for a 42-volt TE system using TE material set #1. The Lp1 designation in Fig. 3 gives the optimized length of the p-type $CeFe_4Sb_{12}$ material, while the Lp2 designation gives the optimized length of the p-type Bi_2Te_3 material. Figure 3 defines the length tradeoff between the two materials in optimized TE designs and demonstrates their strong dependency on T_h. Their dependency on T_c is much less severe, at least in the T_c range investigated. At the maximum power ridge (i.e., approximately T_h = 625 K, see Figure 2, Part I) the optimized p-type $CeFe_4Sb_{12}$ material length is about 0.15 cm, while the p-type Bi_2Te_3 material length is about 0.1 cm. Material tolerance issues could be very important in this region, however, because Fig. 3 shows the optimized length curves vary sharply.

Figure 4 demonstrates the same effects on optimized n-type segment lengths for a 42-volt device design using TE material set #1. The Ln1 designation in Fig. 4 gives the optimized length of the n-type $CoSb_3$ material, while the Ln2 designation gives the optimized length of the n-type Bi_2Te_3.

The TE material area and length tradeoffs shown in Figs. 1-4, with their strong dependencies on T_h, are largely a ramification of the heat exchanger performance and TEPG device interaction that determines T_h and T_c for the TE device. This certainly demonstrates the critical importance of this thermal interaction in the overall system design. This same thermal interaction also strongly impacts the optimized number of TE couples, shown in Fig. 5, for the 42-volt TE device with T_{exh} = 973 K. The optimized number of couples is again sensitive to T_h near the maximum power ridge (i.e., approximately T_h = 625 K, see Figure 2, Part I), significantly impacting device design and optimization in this region.

Before leaving this Device Design Characteristics section, it is informative to also understand the impacts on optimized segment lengths using TE material set #3. Figure 6 shows the optimized p-type segment lengths for the three p-type materials, while Figure 7 shows the optimized n-type segment lengths for the two n-type materials in TE material set #3. In this case, the two low-temperature p-type segments (i.e., Zn_4Sb_3 , Bi_2Te_3 materials) are nearly the same length, with the high- temperature p-type segment (i.e., $CeFe_4Sb_{12}$ material) taking up a majority of the total element length at maximum power. At the peak power ridge, the p-type $CeFe_4Sb_{12}$ segment takes up about 0.13 cm of total length and the remainder of the 0.25 cm total length is split nearly equally between the Zn_4Sb_3 and Bi_2Te_3 materials. The p-type segment lengths are still quite sensitive to T_h near the maximum power ridge (i.e., approximately T_h = 625 K, see Fig. 4, Part I), again significantly impacting device design and optimization in this region. Figure 7 data show the optimized n-type segment lengths are less sensitive to T_h near the maximum power ridge, with the n-type $CoSb_3$ length taking up the majority of the total element length and only a relatively small n-type Bi_2Te_3 length.

Hot-Side / Cold-Side Thermal Resistance Impacts

All analyses to this point have assumed that hot-side and cold-side interface thermal resistances that inherently exist between the heat exchangers and TEPG system are zero. In reality, any heat exchanger/TEPG system will have hot-side and cold-side interfaces manufactured from real-world materials, having non-zero thermal resistance characteristics, providing the thermal coupling between the heat exchanger and TE device. The impact of these thermal resistances on system performance is governed by Eqs. 11 and 12 in Part I.

Interface thermal resistances must be minimized to the extent possible in order to achieve maximum system performance. In addition, these interface thermal resistances must remain within certain allowable limits to maintain viable and stable system performance during operation. System design investigations were performed to quantify allowable cold side interface thermal resistances as a function of available cold side temperature differentials (i.e., $\Delta T_c = T_c - T_{amb}$) and cold side (ambient) mass flow rate, $\dot{m}_c$. Figure 8

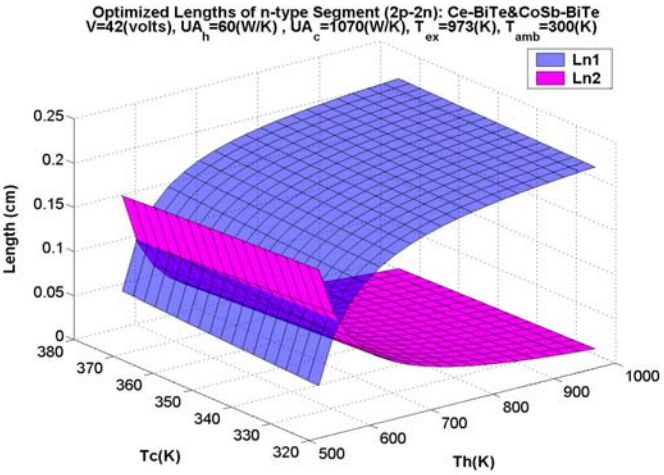

Figure 4 - Optimized n-Type Material Lengths for TE Material Set #1 in a 42-Volt TE Device & T_{exh} = 973 K.

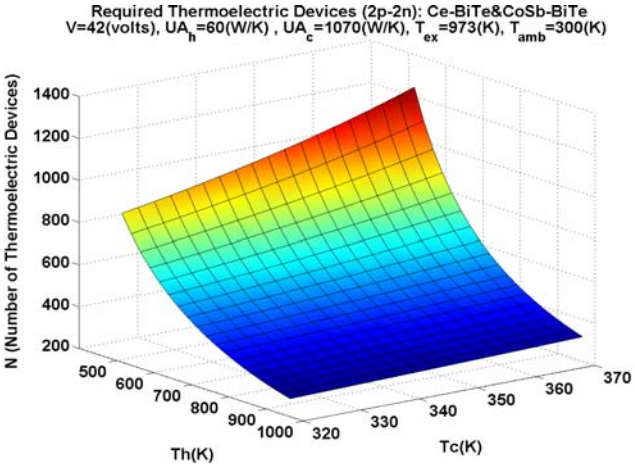

Figure 5 – Optimized Number of Couples for TE Material Set #1 in a 42-Volt TE Device & T_{exh} = 973 K.

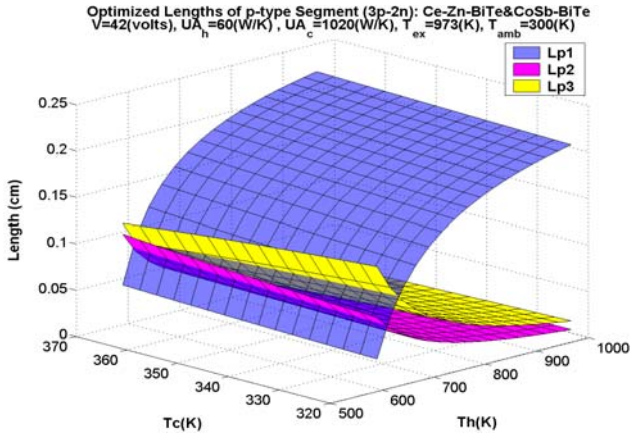

Figure 6 - Optimized p-Type Material Lengths for TE Material Set #3 in a 42-Volt TE Device & T_{exh} = 973 K.

shows maximum allowable cold side resistance at peak power conditions and thermal conditions indicated, for hot side (exhaust gas) mass flow rates of $\dot{m}_h$ = 0.01, 0.02, and 0.03 kg/sec, and TE material combination #1. If cold side mass flow rates, $\dot{m}_c$, are too small for certain available ΔT_c, then the maximum allowable cold side interface thermal resistance

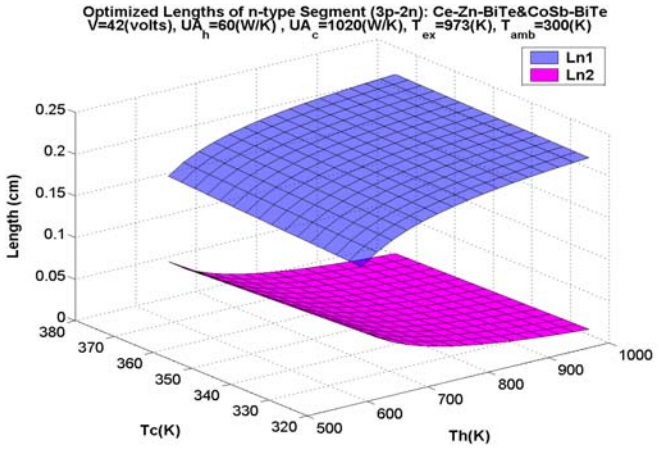

Figure 7 - Optimized n-Type Material Lengths for TE Material Set #3 in a 42-Volt TE Device & T_{exh} = 973 K.

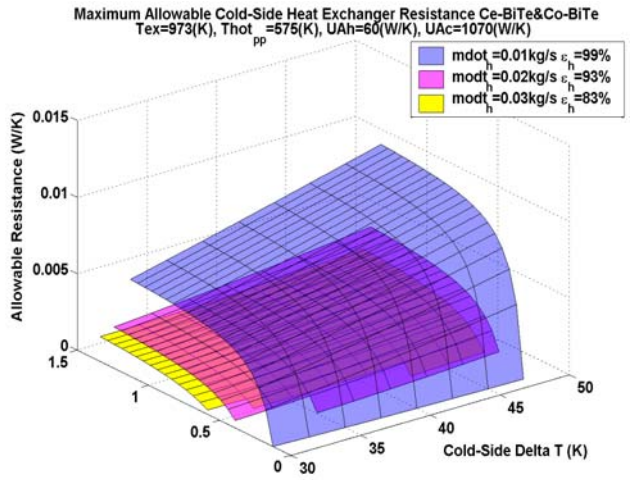

Figure 8 – Allowable Cold-Side Thermal Interface Resistance at Peak Power Conditions in LDP Vehicle Applications Using TE Material Set #1.

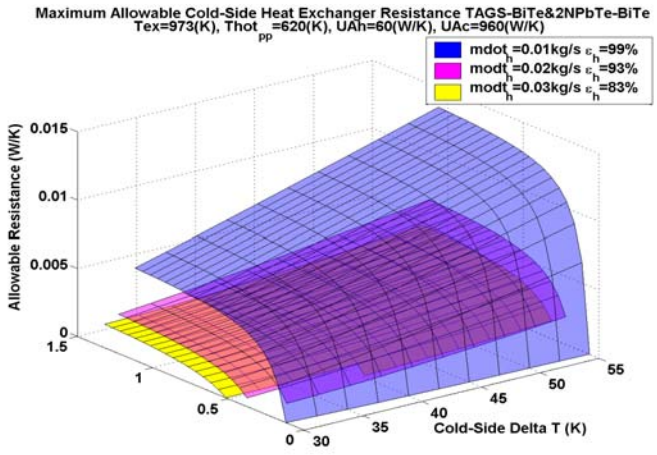

Figure 9 - Allowable Cold-Side Thermal Interface Resistance at Peak Power Conditions in LDP Vehicle Applications Using TE Material Set #2.

that produces stable system performance can indeed be zero. The locus of such critical $\dot{m}_c$ as a function of the available ΔT_c is defined in Fig. 8 for the three $\dot{m}_h$ cases. As the $\dot{m}_c$ increases above these levels for a given cold side temperature differential, the surfaces in Fig. 8 show the sensitivity of allowable cold side interface thermal resistance to $\dot{m}_c$ and available cold side ΔT_c. Allowable interface thermal resistance generally increases as expected as both $\dot{m}_c$ and available cold side ΔT_c increase, however in some cases (i.e., 0.01 kg/sec) this increase can be quite dramatic. The reader should note that these represent maximum allowable cold side interface thermal resistances to maintain thermally stable system performance. Any viable, well engineered system must have interface thermal resistances lower than these limits to maximize system performance over a range of operating conditions.

Figure 9 demonstrates the maximum allowable interface thermal resistances for a heat exchanger / TE system using TE material combination #2. The same effects appear as in the Fig. 8 data using TE material combination #1, but allowable interface thermal resistances are larger. This is because TE systems using TE material combination #2 will operate at higher TE conversion efficiency, therefore creating lower cold side thermal energy dissipation requirements (i.e., lower q_c) for the TE system. This demonstrates an important system design tradeoff to consider between the TE material selection and thermal interface requirements. Better TE materials necessarily make thermal interface design requirements between the heat exchanger and TE device easier to satisfy.

Figure 8 and Fig. 9 data merely set the maximum allowable cold side interface thermal resistances. Cold side mass flow rate required to maintain maximum power output can be strongly dependent on the interface thermal resistance at levels below that shown in Figs. 8 and 9. This is particularly true in high $\dot{m}_h$ cases where a large amount of thermal energy is delivered to the TEPG system, thereby creating larger cold side cooling requirements (i.e., higher q_c). Figure 10 demonstrates the effect of various cold-side interface thermal resistances on required cold-side mass flow rate at different $\dot{m}_h$ levels in TEPG systems with TE material combination #1. At higher $\dot{m}_h$ (0.03 kg/sec), required cold side mass flow rates can be quite sensitive to the cold-side interface thermal resistance, with much higher mass flow rates required if interface thermal resistance is too high. This has serious ramifications on TEPG system designs, particularly in LDP and HD vehicle applications where cooling mass flow can be limited and difficult to deliver to a desired location. If required cold side mass flow rates in Fig. 10 are not maintained in an operating TEPG system, then cold side temperatures will rise and power output will decrease sharply.

Figure 11 shows results from a similar system performance analysis performed for similar $\dot{m}_h$ levels in a TEPG system using TE material combination #2. Similar effects are seen, but required cold-side mass flow rates are

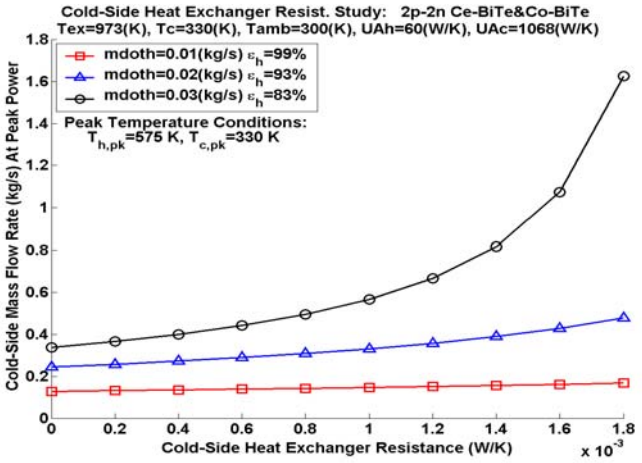

Figure 10 – Cold-Side Thermal Interface Resistance Impacts on Required Cold-Side Mass Flow at Peak Power - TE Material Set #1.

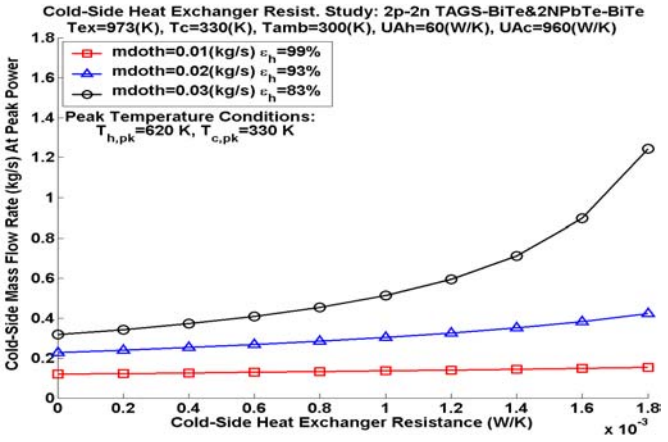

Figure 11 – Cold-Side Thermal Interface Resistance Impacts on Required Cold-Side Mass Flow at Peak Power - TE Material Set #2.

lower using this TE material combination, particularly at higher cold-side interface thermal resistances. The higher performance of TE material combination #2 at given exhaust gas and ambient temperatures was again apparent, resulting in lower cold side heat flow and mass flow requirements. TEPG system analyses in these two figures demonstrate the interrelationship between TE material performance and the required cold side heat exchanger performance in achieving optimum TE system performance. In order to completely optimize the TE system design, it is critical to match TE material performance with heat exchanger performance. Integrated heat exchanger / TEPG system optimization is the only way to identify optimum designs for a given TE material set and achieve truly optimum system performance.

Hot side interface thermal resistances are also critically important in achieving maximum power output in an optimum TEPG system design, because they can fundamentally impact hot side thermal energy transport. This analysis once again was performed for a LDP vehicle (T_{exh} = 973 K) and TEPG system designs using TE material combinations #1 and #2. Figures 12 and 13 show the impact on peak TEPG system power as a function of hot-side interface thermal resistance at various $\dot{m}_h$ levels for TE material combinations #1 and #2, respectively. In both TE material cases, the impact on peak TEPG system power can be quite significant at high $\dot{m}_h$ levels, decreasing power output by approximately 33% as interface resistance increases over the range shown. At intermediate $\dot{m}_h$ levels (0.02 kg/sec), the degradation in power can be approximately 25% as interface resistance increases. These results quantify how critical the hot side thermal interface design (between hot side heat exchanger and TE device) is to system performance in LDP vehicles.

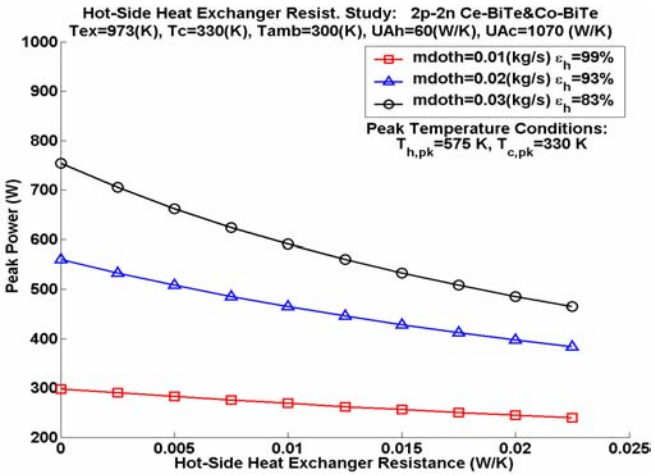

Figure 12 – Hot-Side Thermal Interface Resistance Impacts on System Peak Power - TE Material Set #1.

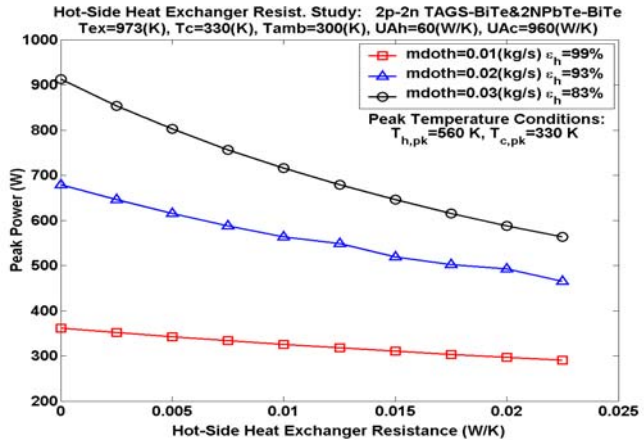

Figure 13 – Hot-Side Thermal Interface Resistance Impacts on System Peak Power - TE Material Set #2.

Thermal Loss Effects on Optimum Device Design

Thermal losses from both the heat exchanger and TEPG device have a critical impact on device design and potential power output in LDP and HD vehicles. Equations 11 and 12 (Part I) define the impact on hot side and cold side thermal flows, and ultimately determine the impact on TE power output and TEPG device design characteristics. System investigations were performed to evaluate TE device design trends and quantify the first–order impacts.

Figure 14 shows the basically linear reduction in TE system peak power from hot-side heat exchanger and TE device thermal losses in an optimized device using TE material set #3, $\dot{m}_h$ = 0.03 kg/sec, and T_{exh} = 973 K. Power loss is quite significant when heat exchanger thermal losses achieve 10% of the hot side thermal input and device losses achieve even 5%, emphasizing the importance of system design to minimize these losses. The same lower thermal input to the TE device that decreases the power output also decreases the required device area in the optimized design.

Figure 15 shows the linear impact of heat exchanger and TE device thermal losses on the TE device total cross-sectional area as associated peak power conditions deteriorate in Fig. 14. The total device cross-sectional area gives a rough idea of the TE device size (i.e., footprint) to generate a given power output. Hot side heat exchanger and TE device thermal losses also noticeably decrease the cold side mass flow rate required to maintain TE device cold side conditions. This helps to relieve somewhat the cold side cooling design challenge for TEPG systems in LDP vehicles, but this is not the preferred design approach.

Figure 16 shows the results of similar thermal-loss-induced peak power degradation in an optimized TE device using TE material set #2. In comparing Fig. 14 power results with those in Fig. 16, it is clear that TE material set #2 actually produces more power than TE material set #3 for the given temperature conditions. The reason for this, given the available temperature conditions, is that there is not sufficient temperature differential to fully exploit the capabilities of the 3-segmented material leg in TE material set #3. Consequently, 2-segmented legs with materials tailored for maximum performance at the specific temperature conditions (i.e., TE materials set #2) will be a better choice when temperature differentials are too small.

Any real, well-engineered TE system will have thermal losses of the order of magnitude shown in Figs. 14-16, so it is critical to understand their impact and magnitude of effect on the TEPG system design. Intelligent design decisions can then be made in the early stages of system design.

TE SYSTEM DESIGN CHARACTERISTICS IN HEAVY VEHICLE APPLICATIONS

Investigations to this point have centered on LDP vehicle requirements (i.e., exhaust gas flow rates and temperatures). Heavy-duty (HD) vehicle applications have much higher exhaust gas flow rates, but slightly lower exhaust gas temperatures, than LDP vehicles. Exhaust gas mass flow rates in a HD vehicle with a 10 Liter, turbo-charged diesel engine are typically in the 0.2–0.4 kg/sec range, and are even higher in some operational drive cycles. HD vehicle exhaust gas temperatures in this case are typically in the 500–550°C range. Kushch et al. [2] have actually reported exhaust mass flow rate and temperature test data for a 1 kW TEPG system slightly higher than these values. Thus, waste thermal energy available for recovery is significantly higher in HD vehicles.

Additional TEPG system performance analyses were conducted to contrast the TE system performance and design requirements for HD vehicles to those of LDP vehicles. Power output, required cold-side mass flow rates, and heat

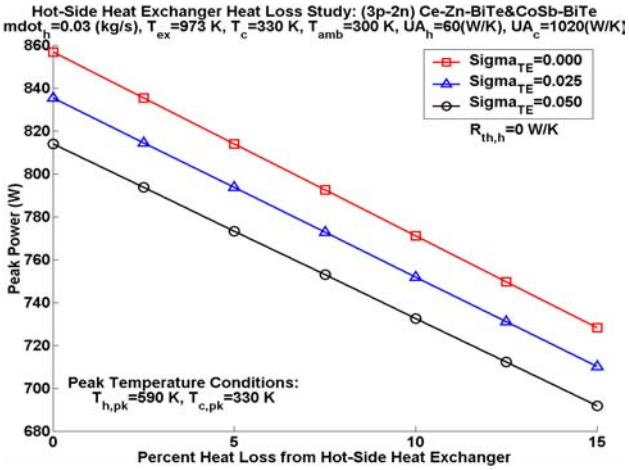

Figure 14 – Thermal Loss Impact on TE Device Peak Power Output for TE Material Set #3 and T_{exh} = 973 K.

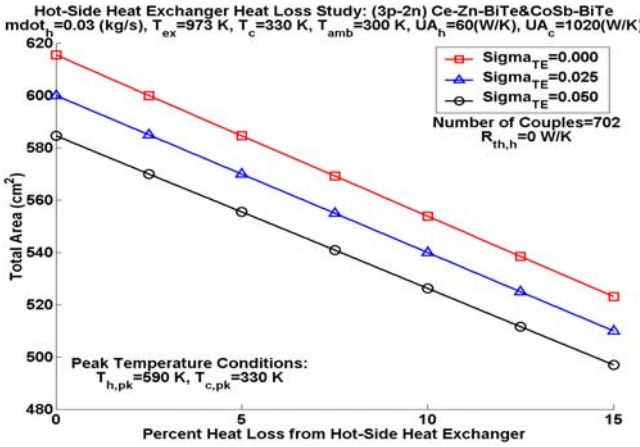

Figure 15 – Thermal Loss Impact on TE Device Total Area Requirement for Peak Power Loss in Figure 14.

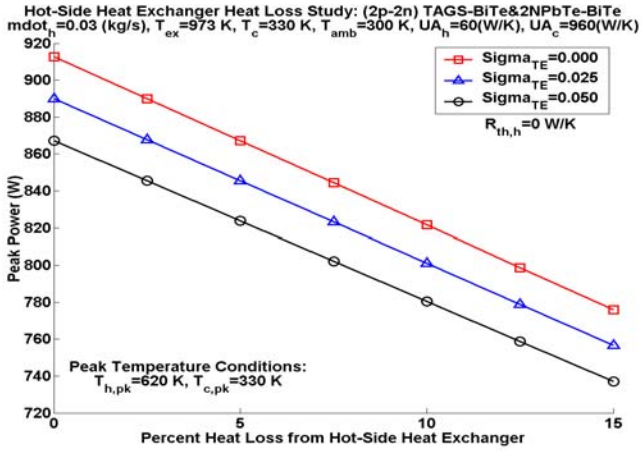

Figure 16 – Thermal Loss Impact on TE Device Peak Power Output for TE Material Set #2 and T_{exh} = 973 K.

exchanger UA requirements were investigated.

Figure 17 displays the power output potentially available for various T_h and T_c combinations and hot side (exhaust gas) mass flow rates of $\dot{m}_h$ = 0.2, 0.3, and 0.4 kg/sec. Figure 17 data demonstrates the same performance tradeoff as in LDP

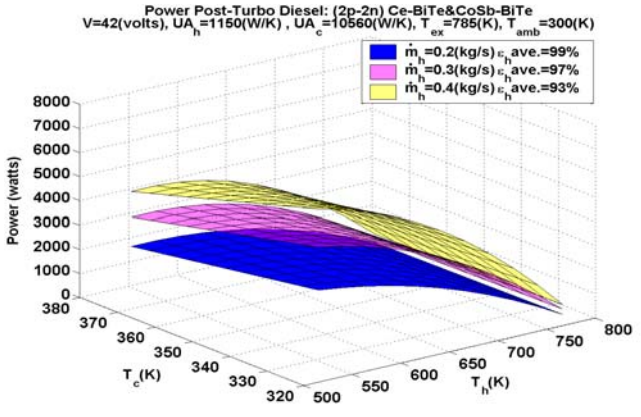

(a)

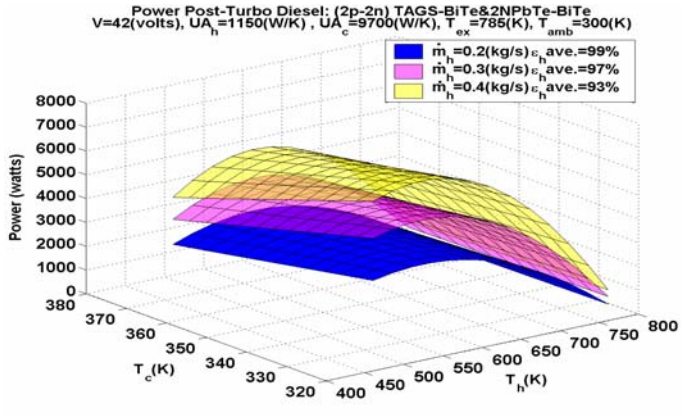

(b)

Figure 17 – Power Output vs. Temperature Conditions and Exhaust Mass Flow Conditions in HD Vehicles Using TE Material Sets #1 and #2.

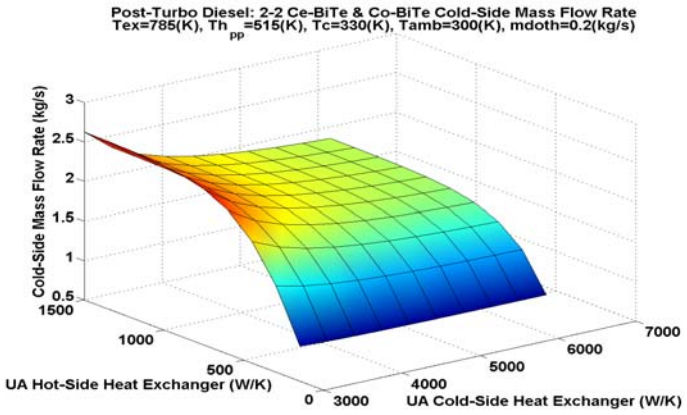

Figure 18 – Required Cold-Side Mass Flow Rate as a Function of Heat Exchanger (UA) Performance in HD Vehicle Applications Using TE Material Set #1.

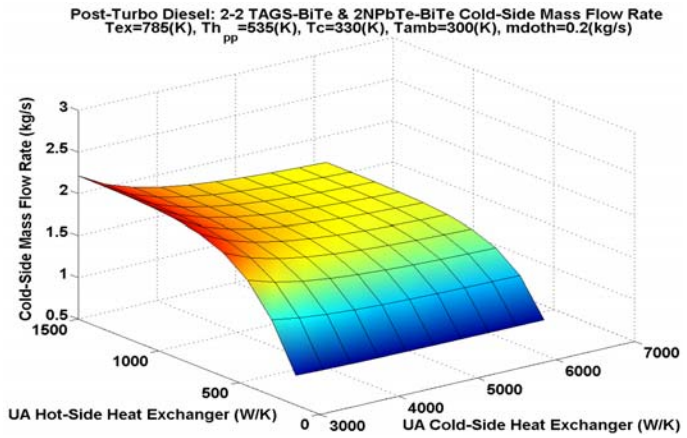

Figure 19 – Required Cold-Side Mass Flow Rate as a Function of Heat Exchanger (UA) Performance in HD Vehicle Applications Using TE Material Set #2.

vehicle data between hot-side heat exchanger performance and TEPG device efficiency in determining the maximum power output conditions. However, the power outputs in HD vehicle applications are much higher than LDP applications, because of the sharply increased $\dot{m}_h$ levels and much larger waste thermal energy available compared to LDP applications. Power outputs up to 5-6 kW appear possible in Fig. 17a for HD vehicles using TE material combination #1. Power outputs exceeding 6 kW are shown in Fig. 17b for HD vehicles using TE material combination #2. This large amount of power available in HD vehicle exhaust streams could have a tremendous impact on research and development planning for HD truck electrification programs at the DOE. Auxiliary power programs at DOE can certainly benefit from advanced TE power systems based on these newly discovered, recently characterized TE materials.

Optimum TE design parameter studies for these HD applications were performed initially for 42-volt systems. However, the optimum design results clearly indicated that a 42-volt TE system is not a very practical system in HD vehicles. It leads to very high current levels, and very high p-leg and n-leg areas, which would create a cumbersome system design. It is clear that higher voltage systems (>~100 volts) are required in HD vehicle applications. Optimized p-segment and n-segment lengths, and their fraction of total element length, were found to be similar to those in LDP vehicle studies presented earlier. This should not pose a serious design challenge in HD applications.

Figure 18 shows the cold-side mass flow rates required by the TEPG system versus the hot-side and cold-side heat exchanger UA values for TE material combination #1. Figure 19 shows the cold-side mass flow rate required by the TEPG system versus the same heat exchanger UA values for TE material combination #2. Compared to LDP vehicle applications, the required heat exchanger UA parameters required for stable TEPG system operation in HD vehicle applications are much higher because of the increased waste thermal energy flows into the device. Cold-side mass flow rates are also much higher than in LDP vehicle applications for the same reason. Consequently, higher performance heat exchanger systems, compared to LDP vehicle cases, will be critical to successfully applying TEPG power systems, and maximizing their power output in HD applications.

The effect of TE material selection on required cold-side mass flow rates also is demonstrated by comparing required mass flow data in Figs. 18 and 19. The superior TE conversion performance of TE material combination #2 reduces the cold-side mass flow rate by a significant 10%-

15%, which may be critical to implementing TEPG systems and achieving stable system performance in HD vehicles.

CONCLUSIONS

Part II of this two-part paper has demonstrated an integrated system analysis approach that allows one to simultaneously quantify effects of important system design parameters on system performance and maximize system power output. Integrated system analyses are providing critical information on how much power is available at various locations in exhaust streams of LDP and HD vehicles.

The interaction of heat exchanger performance and TEPG device performance creates: 1) critical system impacts on maximum TE system power and optimum TEPG system design, 2) important TE system power dependencies on interface thermal resistances and thermal losses, and (3) important impacts on heat exchanger design requirements from TE material selection. TEPG device cross-sectional area is strongly dependent on $\dot{m}_h$, and it increases strongly as T_h increases. Optimum TE element area, segment lengths, and number of couples are sensitive to T_h near the maximum power ridge, creating potential issues regarding material tolerances. Required $\dot{m}_c$ levels to maintain thermal stability and maximum power output can be very sensitive to cold side interface resistances, so cold side design is a critical aspect in TEPG design for LDP and HD waste heat recovery. TE material selection can substantially relax (i.e., reduce) thermal interface design requirements and substantially lower required $\dot{m}_c$ levels. At lower available temperature differentials, TEPG systems with 2-segmented TE couples using properly tailored materials can actually produce more power than 3-segmented TE couple designs. HD vehicles have higher TE power production potential than LDP vehicles by about a factor of 5, with 5-6 kW of electrical energy production possible, but they also have more stringent system design requirements (i.e., heat exchanger UA and required $\dot{m}_c$ levels). This work has: 1) demonstrated that understanding and designing for system interdependencies is crucial to achieving optimum system performance in LDP and HD vehicles, and 2) quantified TE system design effects for some limited LDP and HD exhaust waste-heat-recovery conditions.

ACKNOWLEDGMENTS

The authors would like to thank Dr. Thierry Caillat, NASA-Jet Propulsion Laboratory for thermoelectric property data on skutterudites, Zn_4Sb_3 and Bi_2Te_3 TE materials, and Mr. Norbert Elsner, Hi-Z Technology, Inc. for thermoelectric property data on TAGS and 2N-PbTe TE materials.

REFERENCES

[1] Caillat, T., Fleurial, J.-P., Snyder, G.J., Borshchevsky, A., *Journal of Phys. Chem. Solids*, **7**, 1119 (1997).

[2] Kushch, A.S., Bass, J.C., Ghamaty, S., Elsner, N., Bergstrand, R.A., Furrow, D., and Melvin, M., *Proceedings of 7th Diesel Engine Emission Workshop*, Session 8 – Advanced Diesel Engine Technology, Portsmouth, VA, (2001).